Available online at www.elixirpublishers.com (Elixir International Journal)

Nanotechnology

Elixir Nanotechnology 81 (2015) 31840-31844

ISSN: 2229-712X

Preparation of Ag_2O/PSi/c-Si Heterojunction Device Using Rapid Thermal Oxidation Method for Gas Sensor Application

Asmaa M. Raoof, Lamyaa M. Raoof and Ibrahim R. Agool

Department of Physics, College of Science, Al-Mustansiriyah University, Baghdad, Iraq.

ARTICLE INFO

Article history:

Received: 8 February 2015;

Received in revised form:

28 March 2015;

Accepted: 13 April 2015;

Keywords

Ag_2O,

Rapid thermal oxidation,

Optical properties,

Gas sensor, H_2.

ABSTRACT

The thermal evaporation system type (Edwards) has been used to evaporate high purity (99.9 %) silver on glass substrates at room temperature under low pressure (about 10^{-6} torr) for different thickness (50, 75, 100, 125 and 150) nm. Using a rapid thermal oxidation (RTO) of Ag film at oxidation temperature 350 ^{o}C and different oxidation times, Ag2O thin film was prepared. The optical properties of Ag2O film were investigated and compared with other published results. The gas response behaviors of the p-Ag_2O/PSi/c-Si – based gas sensor to H_2 gas were investigated. The film gas response dependence on the temperature and test gas concentration was tested.

Introduction

Accurate control of oxide thin film synthesis and processing is important in a variety of technological applications including microsensors, microelectronics, and catalysis. Ag_2O, a p-type semiconducting oxide (in contrast to most oxides which are n-type), has been utilized as a thin film sensor [1] and as a high density storage device material [2– 4]. An improved understanding of Ag_2O thin film material properties will aid in achieving improved performance in these applications. Our motivation for examining the growth of Ag and Ag_2O on single crystal sapphire is to explore the structure, stability and chemistry of Ag_2O films for gas sensing applications. Several researchers [5–11] have examined the preparation and properties of silver and silver oxide thin films using a variety of techniques. Typically, films have been grown on substrates which are not crystalline. Pettersson and Snyder [5] grew silver films by r.f. sputtering and electron beam evaporation and then oxidized them in an oxygen plasma from an electron cyclotron resonance (ECR) source. They also deposited oxide films directly using r.f. sputtering of a Ag target in an oxygen background gas. The films were characterized by ellipsometry. Schmidt et al. [6] also oxidized Ag films after growth using an ECR source and examined the optical transmittance of the oxidized films. Hou et al. [7] oxidized Ag films after growth using a glow discharge to create oxygen ions and then examined the fractal structure of the films using transmission electron microscopy. Silver oxide films have been grown directly [8, 9] by reactive electron beam evaporation and DC magnetron sputtering in an oxygen environment. X-ray Diffraction (XRD) measurements indicate that polycrystalline Ag oxide films form with highly preferred (111) orientation when the oxygen flow is high enough. Chiu et al. [10] deposited thin silver oxide films by reactive r.f. magnetron sputtering of metallic Ag in an argon and oxygen environment, followed by annealing under various conditions. The chemistry and structure of the films were examined by XRD, atomic force microscopy (AFM), and X-ray photoelectron spectroscopy (XPS). For annealing temperatures above 500 K, XRD shows polycrystalline Ag_2O films with a strong (101) peak coexisting with a weak (200) peak. Shima and Tominaga [11] grew silver oxide films by r.f. magnetron sputtering in a reactive argon–oxygen environment and characterized them optically and by AFM. Our work continues this research on silver oxide films by emphasizing controlled deposition on high quality single crystal sapphire substrates. The effects of microwave generated oxygen on silver foils have also been investigated [12, 13]. Chou and Phillips [12] studied the influence of O atoms and ions in a plasma on Ag foils. They found that thick Ag_2O films grew for temperature above 350 K. Some AgO was found in films grown at lower temperature based on XRD measurements. The presence of ions accelerated the oxidation rate beyond that observed for O atoms. Bhan et al. [13] exposed Ag foils to atomic oxygen and concluded from XPS and XRD data that only the Ag_2O phase is produced. The role of low coverages of chemisorbed atoms, including oxygen, as a surfactant which helps to achieve two dimensional layer-by-layer growth of Ag films on Ag(111) has been reported [14,15]. Since molecular oxygen has such a low sticking coefficient on Ag (111), it is necessary to maintain an oxygen background pressure of 7.5×10^{-9} Torr in order to observe a small surfactant effect. Monolayer coverages of oxygen have been shown to be effective surfactants for growth of metal films on several metal surfaces [16–18]. The role of the surfactants is believed to be twofold. First they may change the energetics at film island step edges by slowing down the Ag adatom mobility on top of islands and on the substrate and, second, they may slow down the adatom diffusion along the step edges which will enhance interlayer transport [14]. Silver oxide can exist in several phases, with silver (I) oxide (Ag2O) being the most thermodynamically stable. Other phases can exist at low temperature and high oxygen partial pressures [19]. Ag_2O possesses a simple cubic structure with a bulk lattice constant of 0.472 nm at room temperature [20]. AgO usually crystallizes with a monoclinic structure [20] containing both Ag+ and Ag3+ and therefore is more appropriately designated Ag_2O_2. Crystalline Ag has a face centered cubic structure with a bulk lattice constant of 0.409 nm [20]. AgO and Ag_2O can readily be distinguished in XRD and by different peak energy shifts in XPS [10, 21, 22]. Ag_2O thermally decomposes into metallic Ag and O_2. The majority of these decomposition measurements have

Tele:

E-mail addresses: marwa_alganaby@yahoo.com

been done on powder or bulk silver oxide materials and indicate strong decomposition in the range 670–700 K [10, 21–23]. L'vov [24] suggests that the decomposition actually begins around 570 K in vacuum. Fourier transform Infra-red absorbance measurements [25] show evidence for decomposition between 623 and 673 K. XPS measurements [26] also suggest decomposition effects from 593 to 653 K. We report the gas sensor properties of Ag_2O/PSi/c-Si prepared using rapid thermal oxidation method.

Experimental Work

The substrate used was (100) n-type and p-type, single crystal silicon with a resistivity of (0.01-0.02) Ω. cm. These substrates are cut into 1.5×1.5 cm^2 pieces, Initially, the Si wafers were cleaned successively in a sonicating bath with CCl_4, toluene, acetone, ethyl alcohol and 18.5 MΩ-cm deionized water. Electrochemical anodization was performed in dark to produce porous Si layers on polished p-type, (100) oriented Si wafers with a resistivity of 0.01-0.02 Ω. cm and a thickness of ~ 508 µm, using a 1:3 mixture of 48 % HF: 98 % ethanol as an electrolyte. For n-type Si (100) wafers with a resistivity of 0.01-0.02 Ω. cm and a thickness of ~ 508 µm, the etching was carried out in light using a halogen lamp (100W). The anodization was carried out with the distance between the Si substrate to the Pt counter electrode fixed at ~2.5 cm, using a current density of 20 mA/cm^2 for a fixed time of 10 min. PSi layers were fabricated by PECE process for n-type c-Si wafer and by ECE for p-type c-Si wafer. Teflon was used to fabricate the ECE cell that had a circular aperture at the bottom that is sealed with c-Si samples. The cell was a two-electrode system connected to the c-Si samples as the anode and platinum (Pt) as the cathode. The cell was called PECE if the illumination was positioned over the n-type c-Si samples for maximum possible illumination and to generate the required holes for dissolution [27]. In contrast, the cell is called ECE if the p-type c-Si samples were not illuminated. The PECE cell had a circular aperture at the bottom sealed with the c-Si sample. The cell, made of Teflon, was a two-electrode system connected to the c-Si sample as the anode and platinum (Pt) as the cathode. After the anodization, the PSi layers were dried in the following way to reduce the capillary stress using pentane, which has very low surface tension and no chemical reactivity with the PSi layer. The samples were rinsed first with pentane, then with 98 % methanol and finally with deionized water (18.5 MΩ-cm). Next, the samples were dried at about 60 ^oC on a hot plate rather than drying in the N_2 nozzle in order to avoid cracking and peeling of the PSi layer.

High purity (99.99%) Ag thin film was deposited on the (n-PSi and p-PSi) substrates by thermal evaporation system type (Edwards) at 10^{-6} torr. Thickness (100) nm of Ag_2O thin film was grown on (glass, n-PSi and p-PSi) by rapid photothermal oxidation of deposited Ag film using a halogen lamp 350 °C for 90s in static air. The experimental set-up and details are given elsewhere [28]. The ohmic contacts of the device were made by depositing a thick film of Al on the Ag_2O film through special mask.

Results and Discussion

(3-1) Scan Electron Microscope (SEM)

Surface morphologies obtained through Scanning Electron Microscope (SEM) study carried out by (VEGA TESCAN-SEM) in University of Technology at 9.28 kV of Ag_2O films prepared at oxidation temperature 350 ^oC and oxidation time 90 sec with thickness 150 nm. SEM micrograph shows that surface of Ag_2O thin films are smoother as shown in figure (2). The films consist of small particles distributed on the surface that shows Ag films. The color of small particles tends to be dark (nearly black) which reflect the metallic nature of Ag, which typically has dark color as well as the high reflectivity of the obtained film. It can clearly be noticed that the film color is the same as the physical color of the thin metal, so, they look in dark black.

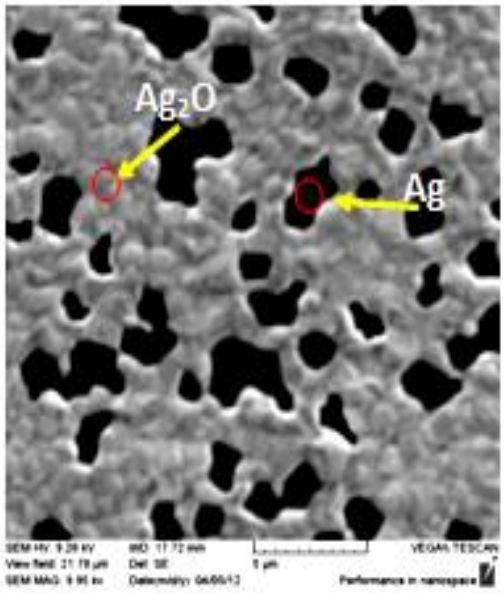

Figure 2. Scan electron microscope of Ag_2O film prepared at 350 ^{o} C and oxidation time) 90 sec

(3-2) Optical Properties

In order to have information on the optical properties of Ag_2O films, transmission (T_r) and absorbance (A) spectra for all films were taken and some optical parameters such as the energy gap (E_g) and absorption coefficient (α) were analyzed by using these spectra. The influence of growth conditions on the optical properties of the prepared films was studied extensively. The transmission of the deposited films on glass substrates was measured and recorded at the ultraviolet and visible regions for the films growth at different thicknesses and oxidation times. Figure (3) (a) shows films without any treatment which represents a purely metal film that has high reflectivities in the visible region. The effect of different thicknesses on the optical properties of the film can be observed in figure (3) (b). The results show an increase in the transmission with decreasing thickness and constant oxidation time and oxidation temperature at a given wavelength. The increase in T_r% is attributed to the well adherent and crystalline nature of the films throughout the coated area, which is obtained due to uniform oxidation and improvement in lattice arrangement, resulting in better optical properties. The improved transmission in the short wavelength region and the peak transmission was in excess of 65% at thickness of 50 nm due to the phase transformation from polycrystalline AgO to Ag_2O, as shown in figure (3) (b).

This result is conditional with many other works [28, 29]. Silver oxide films have a good transparency in the visible region. It is known that the sharp decrease in transparency of Ag_2O films in UV and IR regions is caused by fundamental light absorption and by free-carrier absorption respectively. Figure (3) (c) shows the optical transmission (200-1000) nm as a function of the wavelength for Ag_2O film prepared at different oxidation times and constant thickness and oxidation temperature (350 ^oC). High transmission (50%) was exhibited by films prepared at (150) sec oxidation time, this may be due to the increase in the oxidation which leads to large molecular symmetry (stoichiometry) where Ag_2O films are demonstrated over all other oxide film peaks.

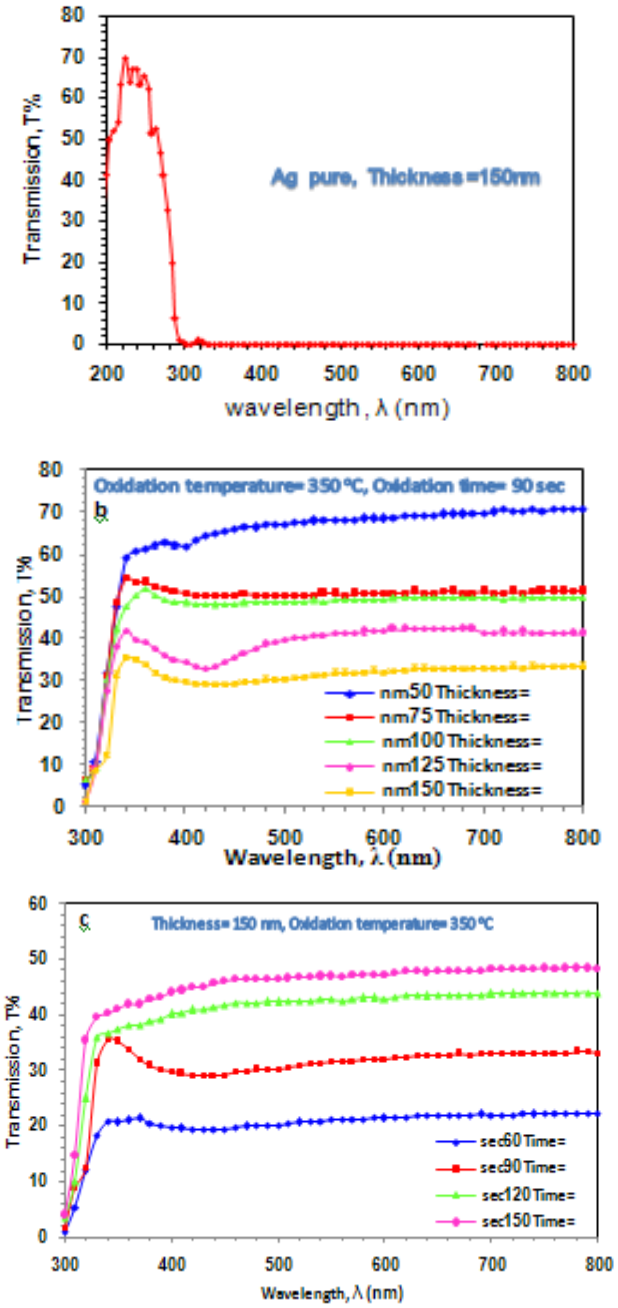

Figure 3. Optical Transmission as a function of wavelength for Ag thin films prepared on glass substrate (a) at room temperature (b) different thickness (c) different oxidation time

In general, it has been found that the transmission of the films were increased when the oxidation time was increased due to film transformation from metal to transparent oxide. The direct optical band gap increases to give a red shift. This shift was due to increase in carrier concentration which results in filling bottom of the conduction band and this filling prevents the transition of the photo generated carriers into the filled levels according to quantum rules and hence leads to far transitions with larger photon energy. This shift is called Burstein -Moss effect. The plot of $(\alpha h\nu)^2$ against (hv) for Ag_2O film prepared at different film thicknesses with 90 sec oxidation time and 350 ^oC oxidation temperature as shown in figure (4), the nature of the plot suggests a direct inter-band transition. The extrapolation of the straight line portion to zero absorption coefficient (α=0) leads to the estimation of band gap energy, it has been found that the photon energy of the films were increased when the thickness of the films increased due to the increasing of the absorption films. It is found that the E_g was about (1.7-2.2) eV and this agrees with the result in a similar work [30].

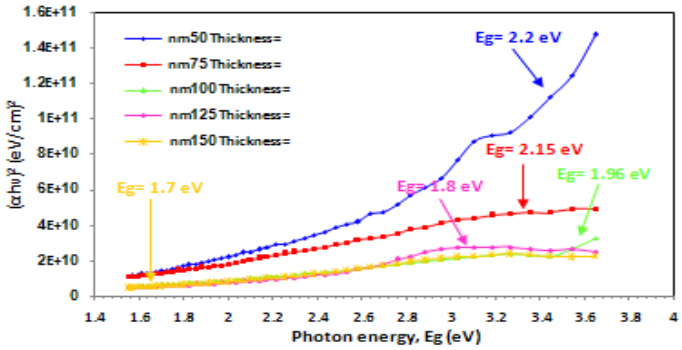

Figure 4. $(\alpha h\nu)^2$ (eV/cm)^2 against hv of Ag_2O films at different film thickness

The structure and lattice parameters of Ag_2O films are analyzed by a LabX XRD 6000 SHIMADZU XR – Diffractometer with Cu Kα radiation (wavelength 1.54059 Å, voltage 30 kV, current 15 mA, scanning speed = 4 °/min) as illustrated in figure (5). The crystallinity of the produced material was characterized using X-ray diffraction (XRD). This technique was also employed by other group which gives an indication about the grain size and formation material type of the prepared thin film. The following figures show the XRD patterns for samples grown at 350 ^oC oxidation temperature and 90 sec oxidation time with different film thickness. At different film thickness (75, 100, 125 and 150 nm) prepared at 90 sec oxidation time and 350 ^oC oxidation temperature as figure (5) (a, b, c and d) show that the structures of films are clearly improved where a significant increase in peak intensity at (111) and (101) planes. This indicates the formation of nearly stoichiometry Ag_2O films.

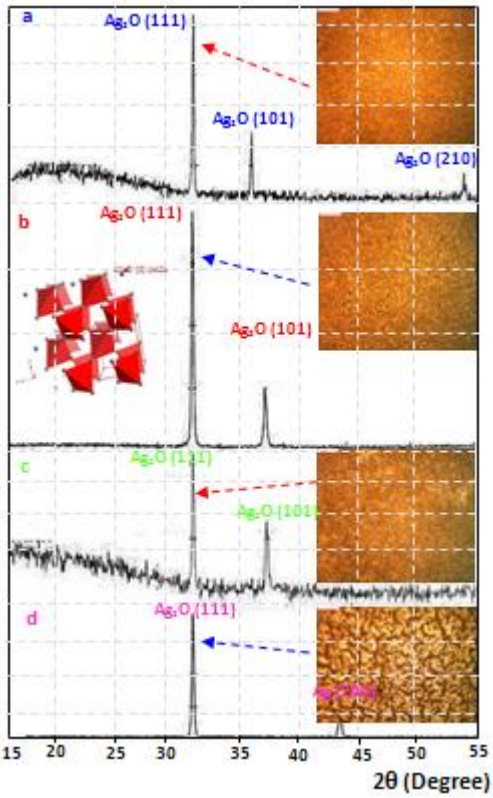

Figure 5. XRD pattern of Ag thin film prepared on glass substrate at 350 ^oC oxidation temperature and 90 sec oxidation time (a) 75 nm, (b) 100 nm, (c) 125 nm and (d) 150 nm

The surface morphology of porous silicon before any heat treatment show in figure (6) (a, b) the poured structure was destroyed; this is related to porous silicon growth mechanism. By electrochemical and photo electrochemical anodization at 20 mA/cm^2 current density for a fixed time of 10 min as shown figure (6) (a, b). The surface morphology of the porous silicon itself changed due to the formation of nano silicon dioxide (SiO_2) and the reduction in porous silicon grain size and roughness. The result shows a uniform net work like porous surface with a root mean squire value (45.2 nm) that revealed low roughnesses of about (35.7 nm) which insure homogeneity in pore size values, comparing with figure (6) (b) where the RMS was (23.4 nm) and the roughness about (18.6) the increase in its value on first case related to the re-distribution of oxide atoms on the porous surface and also associated with the increase in the average grain size (from 327.52 to 346.44 nm). The obtained films display smooth, uniform grain size and void free, i.e., very limited NO. of droplets were observed.

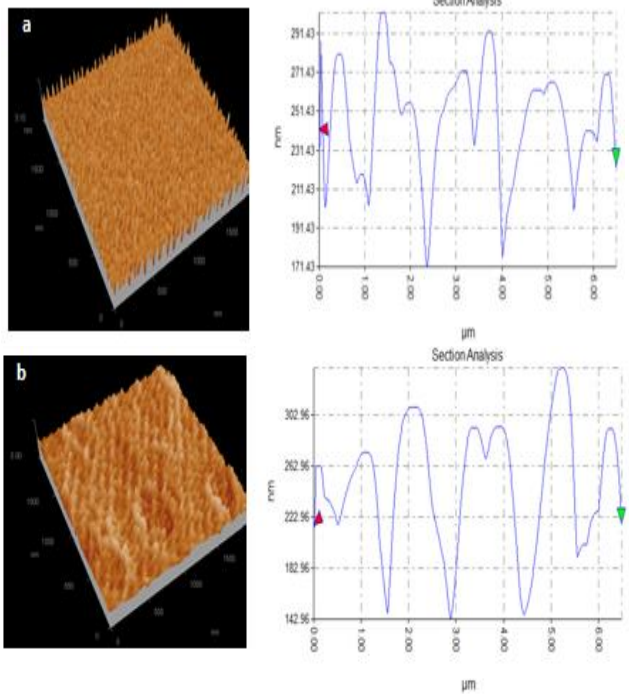

Figure 6. Surface morphology of (a) p- type porous silicon and (b) n- type porous silicon prepared at current density 20 mA/cm^2 and time of 10 min

The dependence of the gas response of p-Ag_2O/p-PSi/c-Si and p-Ag_2O/n-PSi/c-Si heterojunction devices on the H_2 concentration at an operating temperature 250 ^oC is shown in figure (7) as the following equation:

$$Sensitivity(\%) = \left|(R_{gas} - R_{air})/R_{air}\right| \times 100$$

where Ra is the resistance in air and Rgas is the resistance in a sample gas. It is observed that the gas response increases as the H_2 concentration increases from 100 to 400 ppm. The low gas concentration implies a lower surface coverage of gas molecules, resulting into lower surface reaction between the surface adsorbed oxygen species and the gas molecules. The increase in the gas concentration increases the surface reaction due to a large surface coverage. Further increase in the surface reaction will be gradual when saturation of the surface coverage of gas molecules is reached. Thus, the maximum gas response was obtained at an operating temperature of 250 ^oC for the exposure of 400 ppm of H_2. p-Ag_2O/p-PSi/c-Si and p-Ag_2O/n-PSi/c-Si heterojunction devices are able to detect up to 100 ppm for H_2 with reasonable gas response at an operating temperature 250 ^oC.

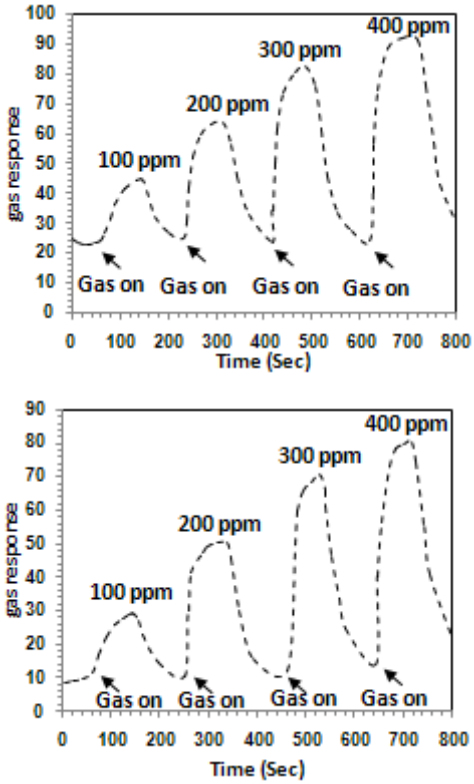

Figure 7. Dependence of the gas response on the H_2 concentration at 250 ^oC of (a) p-Ag_2O/p-PSi/c-Si and (b) p-Ag_2O/n-PSi/c-Si heterojunction devices

Conclusions

The structural properties of undoped polycrystalline Ag2O thin film prepared at different film thickness and oxidation times by using rapid thermal oxidation technique. The transmittance T in the visible and NIR was investigated; the allowed direct energy gap was determined to be 1.96 eV at optimum condition of 350 ^oC and 90 s. The dependence of the resistivity on the film thickness and oxidation time has been studied. The gas response behaviors of the p-Ag_2O/PSi/c-Si – based gas sensor to H_2 gas were investigated. The film gas response dependence on the temperature and test gas concentration was tested.

References

[1] N. Yamamoto, S. Tonomura, T. Matsuoka, H. Tsubomura, Jpn. J. Appl. Phys. 20 (1981) 721.
[2] S. Haratani, J. Tominaga, H. Dohl, S. Takayama, J. Appl. Phys. 76 (1994) 1297.
[3] J. Tominaga, D. Buchel, C. Mihalcea, T. Shima, T. Fukaya, Mater. Res. Soc. Symp. Proc. 728 (2002) 179.
[4] F.H. Wu, H.-P.D. Shieh, Jpn. J. Appl. Phys. Part 1 42 (2003) 820.
[5] L.A.A. Pettersson, P.G. Snyder, Thin Solid Films 270 (1995) 69.
[6] A.A. Schmidt, J. Offermann, R. Anton, Thin Solid Films 281/282 (1996) 105.
[7] S.M. Hou, M. Ouyang, H.F. Chen, W.M. Liu, Z.Q. Xue, Q.D. Wu, H.X. Zhang, H.J. Gao, S.J. Pang, Thin Solid Films 315 (1998) 322.
[8] U.K. Barik, A. Subrahmanyam, in: V. Kumar, P.K. Basu (Eds.), Proceedings of the 11th International Workshop on Physics of Semiconductor Devices, New Dehli, India, Dec. 11 – 15, 2000, SPIE, vol. 4746, 2002, p. 1271.
[9] U.K. Barik, S. Srinivasan, C.L. Nagendra, A. Subrahmanyam, Thin Solid Films 429 (2003) 129.
[10] Y. Chiu, U. Rambabu, M.-H. Hsu, H.-P.D. Shieh, C.-Y. Chen, H.-H. Lin, J. Appl. Phys. 94 (2003) 1996.

[11] T. Shima, J. Tominaga, J. Vac. Sci. Technol., A, Vac. Surf. Films 21 (2003) 634.
[12] C.H. Chou, J. Phillips, J. Vac. Sci. Technol., A, Vac. Surf. Films 9 (1991) 2727.
[13] M.K. Bhan, P.K. Nag, G.P. Miller, J.C. Gregory, J. Vac. Sci. Technol., A, Vac. Surf. Films 12 (1994) 699.
[14] J. Vrijmoeth, H.A. van der Vegt, J.A. Meyer, E. Vlieg, R.J. Behm, Phys. Rev. Lett. 72 (1994) 3843.
[15] H.A. van der Vegt, W.J. Huisman, P.B. Howes, T.S. Turner, E. Vlieg, Surf. Sci. 365 (1996) 205.
[16] R. Moroni, F. Bisio, A. Gussoni, M. Canepa, L. Mattera, Surf. Sci. 482– 485 (2001) 850.
[17] M. Onishi, L. Li, S. Toril, A. Kida, M. Doi, M. Matsui, Mater. Trans. 43 (2002) 2143.
[18] D.J. Larson, A.K. Peford-Long, A. Cerezo, S.P. Bozeman, A. Morrone, Y.Q. Ma, A. Georgalakis, P.H. Clifton, Phys. Rev., B 67 (2003) 144420– 144421.
[19] J. Assal, B. Hallstedt, L.J. Gauckler, J. Am. Ceram. Soc. 80 (1997) 3054.
[20] R.W.G. Wyckoff, 2nd ed., Crystal Structures, vol. 1, Wiley, New York, 1963.
[21] W.A. Parkhurst, S. Dallek, B.F. Larrick, J. Electrochem. Soc. 131 (1984) 1739.
[22] S. Dallek, W.A. West, B.F. Larrick, J. Electrochem. Soc. 133 (1986) 2451.
[23] S. Dallek, W.A. Parkhurst, B.F. Larrick, Thermochim. Acta 78 (1984) 333.
[24] B.V. L'vov, Thermochim. Acta 333 (1999) 13.
[25] G.I.N. Waterhouse, G.A. Bowmaker, J.B. Metson, Phys. Chem. Chem. Phys. 3 (2001) 3838.
[26] G. Scho¨n, Acta Chem. Scand. 27 (1973) 2623.
[27] V. Lehmann, 1993 , J. Electrochem. Soc. , 140, 2836.
[28] MC. Arenas, H. Hu, A. Scanchez, 2006, Sol. Energy Mater. Sol. Cells, 90, 2431.
[28] Xiao-Yong Gao, Hong-Liang Feng, Zeng-Yuan Zhang, Jiao-Min Ma, Meng-Ke Zhao, Chao Chen, Jin-Hua Gu, Shi-E Yang, Yong-Sheng Chen and Jing-Xiao Lu, " Effect of the Oxygen Flux Ratio on the Structural and the Optical Properties of Silver-oxide Films Deposited by Using the Direct-current Reactive Magnetron Sputtering Method", Journal of the Korean Physical Society, Volume 58, Number 2, Pages 243_247, February 2011.
[29] Yi Chiu, "Fabrication And Nonlinear Optical Properties Of Nanoparticle Silver Oxide Films", Department of Electrical and Control Engineering, National Chiao Tung University, 1001 Ta Hsueh Road, Hsinchu 300, Taiwan, Republic of China, Volume 94, Number 3, 2003.
[30] Bocka. F. X., Christensenb. T. M., Riversc. S. B., Doucettea. L. D. and Lad. R. J., "Growth and structure of silver and silver oxide thin films on sapphire", Thin Solid Films, Volume 468, Pages 57– 64, 2004.